JOURNAL OF MATERIALS SCIENCE 25 (1990) 4488–4494

Mechanical properties of a transformation-toughened glass-ceramic

G. L. LEATHERMAN
Mechanical Engineering Department, Worcester Polytechnic Institute, Worcester, Massachusetts 01609, USA

M. TOMOZAWA
Materials Engineering Department, Rensselaer Polytechnic Institute, Troy, New York 12180-3590, USA

The fracture toughness of a transformation-toughened glass-ceramic containing 12 vol% t-ZrO_2 was measured. Heat-treatment conditions were selected to produce from the same glass composition a glass-ceramic which contained 12 vol% m-ZrO_2 in a nearly identical matrix. The transformation-toughened material was found to have a fracture toughness 65% greater than the m-ZrO_2-containing material at room temperature. However, at 77 K both materials were found to have approximately the same fracture toughness. Additionally, the susceptibility of the two glass-ceramics to fatigue was determined. No improvement in fatigue behaviour of the transformation-toughened glass-ceramic over the other glass-ceramic was observed.

1. Introduction

Dramatic increases in the toughness of certain ceramic materials have been realized by the incorporation of tetragonal zirconia (t-ZrO_2) particles into these materials. Partially stabilized zirconia [1], alumina [2], SiC [3], and several other traditional ceramics have been toughened in this manner [4, 5]. Although other toughening mechanisms may also be active, the stress-induced martensitic transformation of t-ZrO_2 particles (tetragonal to monoclinic) plays a significant role in increasing the toughness of these materials. The increment of toughening increase has been determined to be given by [6, 7]

$$K = 0.22 V_t \varepsilon^T E d^{1/2}/(1 - \nu) \quad (1)$$

where V_t is the volume fraction of transformable t-ZrO_2, ε^T is the dilational strain associated with the transformation, d is the size of the transformation zone around the crack, E is Young's modulus, and ν is Poisson's ratio. The actual difference in toughness between similar transformation-toughened and non-transformation-toughened materials is usually around a factor of 2 or 3.

Until quite recently, interest in utilizing transformation toughening in glass-ceramics (crystalline ceramics produced by the controlled crystallization of glasses) has been surprisingly lacking even though ZrO_2 is used in many glass-ceramic compositions as a nucleating agent [8–11]. Tetragonal zirconia also appears as a distinct phase upon crystallization in many glass-ceramics [12–15].

Nogami and Tomozawa [16] have examined transformation toughening in zirconia–silica binary glass-ceramics produced by sol–gel techniques. Keefer and Michalske [17] have studied transformation toughening with synchrotron radiation measurements of transformation zone depths on a 15% ZrO_2 · 13% Na_2O · 72% SiO_2 (mol%) glass-ceramic which contained ~2.5 vol% t-ZrO_2 upon crystallization and an 11% ZrO_2 · 11% Li_2O · 16% B_2O_3 · 62% SiO_2 (mol%) glass-ceramic which contained ~10 vol% combined t- and m-ZrO_2 upon crystallization. Transformation toughening has been examined in an MgO–Al_2O_3–SiO_2–ZrO_2 glass-ceramic produced by crystallization of sintered glass frit [18], and recently, a cordierite glass-ceramic was toughened by the addition of t-ZrO_2 particles to the glass frit prior to sintering [19].

This paper examines transformation toughening in a glass-ceramic based on the following composition (mol%): 13% ZrO_2–30% Li_2O–4% TiO_2–53% SiO_2. The composition was selected from the detailed investigation of the melting and crystallization characteristics of the Li_2O–SiO_2–ZrO_2 system [20]. Heat-treatment conditions were selected to produce a glass-ceramic which contained 12 vol% t-ZrO_2 and one which contained 12 vol% m-ZrO_2 in nearly identical matrices. The mechanical properties of these two glass-ceramics are compared, and the results are discussed in the light of current toughening models.

2. Experimental procedure

2.1. Materials

Glass of composition (mol%) 13% ZrO_2–30% Li_2O–4% TiO_2–53% SiO_2 was produced by combining the appropriate amounts of reagent grade oxides or carbonates (Zircon, $ZrSiO_4$, was the source of zirconia) in 100 g batches. The raw materials were mixed in ethanol with a mortar and pestle. After drying, the components were melted in an open platinum crucible

0022–2461/90 $03.00 + .12

in air at 1600° C for 4 h. The melts were stirred several times using a platinum stir-rod to ensure homogeneity. Melts were poured into a brass mould. The glass was annealed at 500° C for 1 h then furnace cooled to room temperature.

Specimens were cut from the annealed glass (2.5 cm × 2.5 cm × 0.5 cm plates for indentation tests and general analysis and 0.5 cm × 0.5 cm × 5 cm beams for four-point bend testing) using a low-speed saw with a diamond wafering blade. The specimens were polished using 240 grit SiC then given the appropriate thermal treatment to produce the desired glass-ceramic. Both glass-ceramics received identical nucleation treatments at 615° C for 15 h. The glass-ceramic containing t-ZrO_2, labelled ZT5-T, was crystallized at 810° C for 3 h; the glass-ceramic containing m-ZrO_2, labelled ZT5-M, was crystallized at 975° C for 30 min. The crystallization behaviour of the base glass has been reported elsewhere [20].

2.2. X-ray diffraction

The glass-ceramics were characterized by X-ray diffraction with a diffractometer utilizing CuK_α radiation (wavelength = 0.154 18 nm). The X-ray tube was operated at 1.575 kW. A graphite crystal monochromator was employed.

2.2.1. Quantitative analysis

Quantitative phase analysis was done using standards. Standard samples for the quantitative analysis of tetragonal and monoclinic zirconia were prepared by mixing varying amounts zirconia powder of known tetragonal/monoclinic ratio with uncrystallized ZT5 glass powder. The relationship established by Toraya *et al.* [21] was used to determine the relative amounts of tetragonal and monoclinic zirconia

$$V_m = 1.311X_m/(1 + 0.311X_m) \quad (2)$$

where V_m is the volume fraction of monoclinic zirconia. The mole fraction of monoclinic zirconia, X_m is given by

$$X_m = [I_m(1\,1\,1) + I_m(1\,1\,\bar{1})]/[I_m(1\,1\,1) + I_m(1\,1\,\bar{1}) + I_t(1\,1\,1)] \quad (3)$$

where $I_m(h\,k\,l)$ or $I_t(h\,k\,l)$ is the integrated intensity of the respective monoclinic or tetragonal peak. Standards for the other crystalline phases present were produced in a like manner.

Quantitative analysis was performed primarily on bulk samples rather than on powder samples in order to avoid transformation of tetragonal zirconia to monoclinic zirconia induced by comminution. There is a difference in packing factor (density) between bulk and powder specimens of the same material and consequently a difference in diffracted intensity. This change was determined and used in determining a scaling factor that enabled direct analysis of bulk samples from powder standards.

2.2.2. X-ray peak broadening

The average t-ZrO_2 crystallite size of ZT5-T was determined by X-ray peak broadening. Data were collected by step-scanning over the angular range of the peak in question at intervals of 0.02° 2θ. The data acquisition time at each 0.02° interval was between 30 and 120 sec depending on the intensity of the peak. The data were entered into a computer for subsequent analysis.

Extracting useful information from X-ray peak broadening is a two-step task requiring first the separation of machine broadening from the pure breadth and then analysing the pure breadth to determine crystallite size and strain.

The machine broadening, $g(2\theta)$, and the pure breadth, $f(2\theta)$, are related to the actual diffraction profile, $h(2\theta)$, by the following convolution relation [22]

$$h(2\theta) = \int_{-\infty}^{\infty} g(2\theta)\, f(2\theta - \phi)\, d\phi \quad (4)$$

where 2θ is the diffraction angle, and ϕ is a variable of integration. Application of the above convolution integral shows that for all three profiles being Cauchian

$$B = b + \beta \quad (5)$$

where B is the full-width at half maximum (FWHM) of the observed profile, b is the FWMH of the machine broadening profile, and β is the FWHM of the pure profile. The pure breadth can then be obtained simply by subtracting the FWHM of the machine broadening contribution (obtained by diffracting a strain-free, large grain-size reference material) directly from the observed peak FWHM. Although most real profiles are not entirely Cauchian, this approximation does not produce excessive error in the case of zirconia [12, 22].

The machine broadening profile was determined using a polycrystalline α-quartz sample with grain size greater than 10 μm. Full-width at half maximums were corrected for the $K\alpha_1$ $K\alpha_2$ doublet by fitting the actual profiles to the sum of two Cauchy functions using a non-linear least squares fitting routine. It was assumed that the $K\alpha_1$ and $K\alpha_2$ profiles were identical Cauchy functions and that the $K\alpha_2$ profile is one-half the intensity of the $K\alpha_1$ profile and shifted from the $K\alpha_1$ towards larger angles by

$$\delta 2\theta = 2(\delta\lambda/\lambda) \tan\theta \quad (6)$$

where $\delta\lambda$ is difference in wavelength between $K\alpha_1$ and $K\alpha_2$ and λ is the wavelength of $K\alpha_1$. Fig. 1 shows the fit for the (1 0 1) peak for α-quartz used to determine machine broadening and Fig. 2 shows a fit for the (1 1 1) peak of t-ZrO_2 from ZT5-T.

X-ray line broadening of a specimen, in general, originates from both small crystal size and strain or defects. The presence of broadening due to strain or defects in t-ZrO_2 was determined by plotting $\beta \cos\theta$ against $\sin\theta$. For this purpose the (1 1 1), (2 0 0), and the (3 1 1) profiles were employed. If a straight line results, the slope is proportional to the root mean squared (r.m.s.) strain in the crystallites [22]. A horizontal line indicates no r.m.s. strain. A non-linear relationship is the result of the presence of defects such as stacking faults. Fig. 3 shows plots of $\beta \cos\theta$ against $\sin\theta$ for t-ZrO_2 in crystallized ZT5 glass from a variety of crystallization treatments. They all resulted

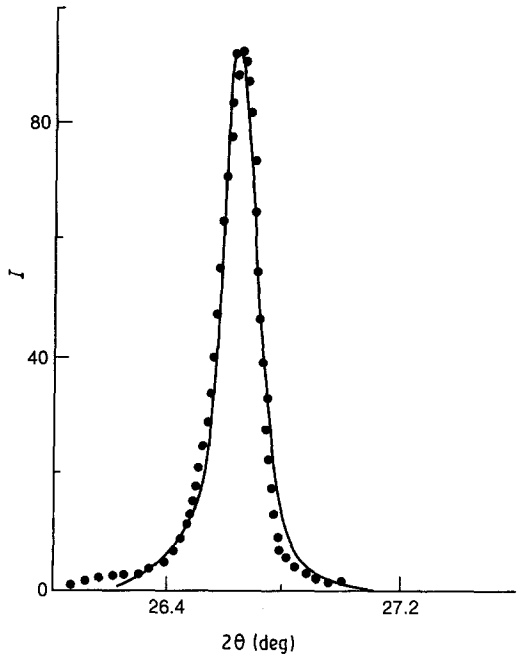

Figure 1 Comparison of α-quartz (1 0 1) peak shape with computer-generated Cauchian fit. The points are actual data, the solid line is the computer-generated fit.

in horizontal lines indicating that peak broadening of t-ZrO_2 is due to crystallite size alone in this system.

The pure $K\alpha_1$ FWHM, β, of the (1 1 1) of t-ZrO_2 so obtained was used in Scherer's equation (assuming spherical particles) to obtain the average crystallite size

$$D_m = 0.89\ \lambda/\beta \cos \theta \quad (7)$$

2.2.3. Transformation-zone size determination

The transformation-zone size for ZT5-T was estimated from fracture surfaces using the two-X-ray wavelength

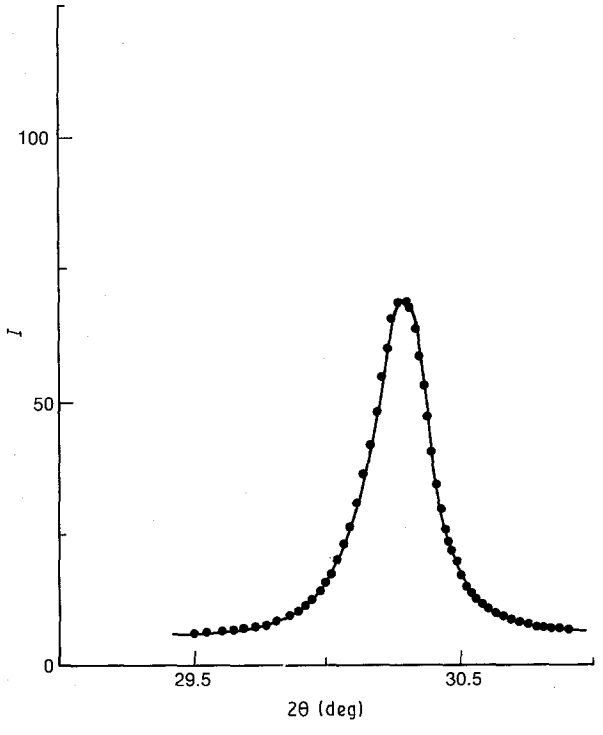

Figure 2 Comparison of t-ZrO_2 (1 1 1) peak shape with computer-generated Cauchian fit. The points are actual data, the solid line is the computer-generated fit.

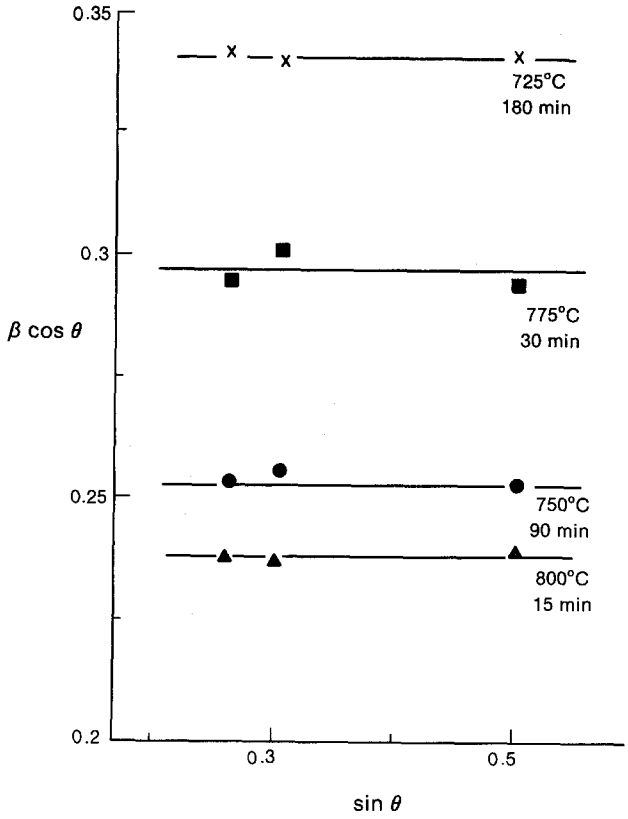

Figure 3 Plot of $\beta \cos \theta$ against $\sin \theta$ for t-ZrO_2 in crystallized ZT5 glass after a variety of crystallization treatments. Crystallization time and temperature are shown.

technique of Garvie *et al.* [23]. The volume fraction of monoclinic ZrO_2 at the fracture surface of a diffraction specimen is given by

$$V_m = X_m [1 - \exp(-2\mu d/\sin \theta)] \quad (8)$$

where X_m is the mole fraction of material transformed to monoclinic by the passage of the crack, d is the transformation zone depth, and μ is the X-ray linear absorption coefficient of the material. This contains two unknowns, the fraction of material transformed and the zone depth. However, by using two different X-ray wavelengths the following ratio eliminates X_m

$$V_{m1}/V_{m2} = [1 - \exp(-2\mu_1 d/\sin \theta_1)]/[1 - \exp(-2\mu_2 d/\sin \theta_2)] \quad (9)$$

Thus by determining the monoclinic content on the fracture surface using two X-ray wavelengths and knowledge of the linear absorption coefficients the transformation zone depth can be determined. Cr$K\alpha$ was used as the second wavelength in this study.

2.3. Mechanical properties

Fracture toughness, K_{Ic}, was determined using single-edged notched beam (SENB) specimens in four-point bending (outer span 3.17 cm, inner span 1.91 cm). The specimens were notched after crystallization. Tests were conducted at room temperature, 25° C, and at 77 K in liquid nitrogen. Specimens were coated with paraffin oil for room-temperature tests. A cross-head speed of 2.54 cm min^{-1} was used.

In order to confirm some of the results of the above tests, indentation fracture toughness measurements were also made on both glass-ceramics. Vickers

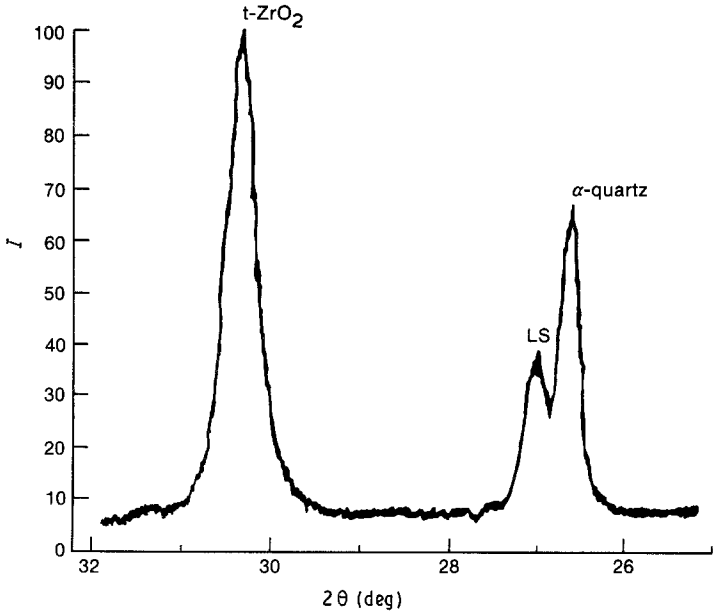

Figure 4 X-ray diffraction pattern of ZT5-T.

indentations were made under both paraffin oil and water. An indentation load of 196 N was used. Immediately after indentation the resulting crack patterns were examined by scanning electron microscopy, and the crack lengths were determined from scanning electron micrographs. Relative K_{Ic} values were determined using the equation of Lawn and Fuller [24] for a Vickers indentation and half-penny-shaped cracks

$$K_{Ic} = P(\pi c)^{3/2} \tan 68° \quad (10)$$

where P is the indentation load and c is the half-penny crack radius. In all cases c was greater than or equal to twice the indentation half-diagonal.

Elastic moduli were determined by the ultrasonic pulse transmission technique [25]. Densities were determined by Archimedes' method.

3. Results and discussion

3.1. Characterization

Glass-ceramic ZT5-T, as previously mentioned contains 12 vol % t-ZrO_2. The average t-ZrO_2 crystallite size as determined by X-ray peak broadening is 37 nm. The distribution of phases as determined by quantitative X-ray diffraction is (wt %): 26% t-ZrO_2, 45% lithium metasilicate ($Li_2O \cdot SiO_2$), 22% α-quartz, and the balance residual glass. The X-ray diffraction pattern of ZT5-T is shown in Fig. 4.

Glass-ceramic ZT5-M, as also previously mentioned, contains 12 vol % m-ZrO_2. The distribution of phases is (wt %): 25% m-ZrO_2, 45% lithium metasilicate ($Li_2O \cdot SiO_2$), 10% α-quartz, and the balance residual glass. The X-ray diffraction pattern of ZT5-M is shown in Fig. 5.

The matrices of the two glass-ceramics are quite similar; the only difference is the amount of α-quartz which has crystallized from the residual glass. Microstructurally they are also quite similar. They both consist of spherulites of lithium metasilicate surrounded by quartz/residual glass. Fig. 6 shows both microstructures as well as typical indentation patterns. The similarity between the two glass-ceramics can also be seen in the close agreement in other properties. Several

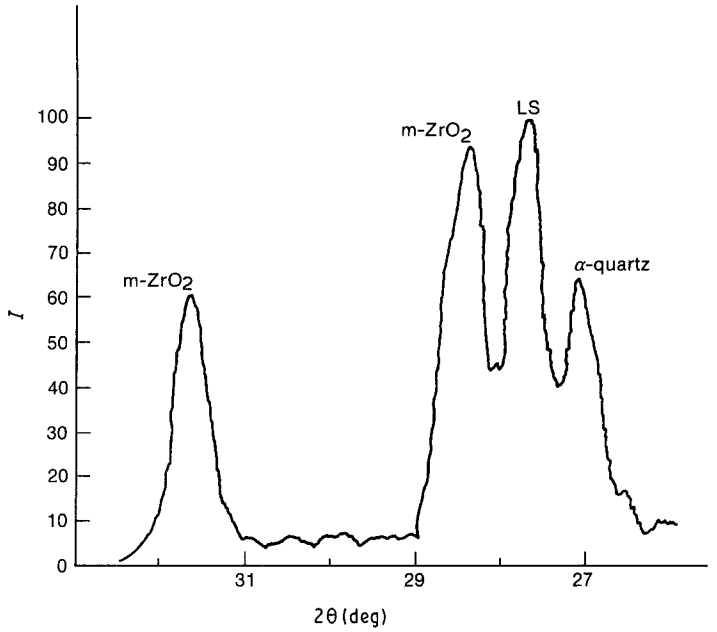

Figure 5 X-ray diffraction pattern of ZT5-M.

TABLE I Selected properties of the glass-ceramics used in this study

Glass-ceramic	Young's modulus, E (GPa)	Shear modulus, G (GPa)	Poisson's ratio, ν	Density, ρ (g cm^{-3})
ZT5-T	108	44	0.22	2.87
ZT5-M	105	44	0.19	2.84

of these are shown in Table I. The elastic moduli are quite close in value and only small differences exist in density.

3.2. Fracture toughness

The room-temperature fracture toughness (SENB) of ZT5-T is 2.29 MPa m$^{1/2}$. That of ZT5-M is 1.39 MPa m$^{1/2}$. This suggests that transformation toughening is indeed occurring. This will be discussed further in a subsequent section. At 77 K the K_{Ic} of ZT5-M increases slightly to 1.50 MPa m$^{1/2}$. This increase might be expected because fatigue may be operative at room temperature but not at 77 K. Surprisingly, the fracture toughness of ZT5-T decreases substantially at 77 K to 1.64 MPa m$^{1/2}$. X-ray diffraction (at room temperature) of the specimens tested at 77 K revealed that approximately 8% (1 total vol %) of the t-ZrO_2 had transformed to m-ZrO_2. X-ray diffraction patterns before and after exposure to liquid nitrogen appear in Fig. 7. To elucidate whether the decrease in K_{Ic} was due to this transformation, a series of ZT5-T samples were cooled in liquid nitrogen and then tested at room temperature. The measured fracture toughness of this group was 1.59 MPa m$^{1/2}$. It would appear that the decrease in toughness is associated with the transformation. Although some reduction in toughness results directly from decreasing the amount of transformable ZrO_2 from 12% to 11%, estimations based on Equation 1 show that the loss of 1 vol % transformable t-ZrO_2 cannot be responsible for the total decrease in toughness. Another source of the decrease must be found. A likely candidate is weakening due to microcracks formed by the transformation. The fracture toughness data are summarized in Table II.

3.3. Fatigue

The effect of transformation toughening on the susceptibility to water-enhanced fatigue in this system was evaluated by comparing the indentation fracture toughness of both glass-ceramics in water and in paraffin oil. Any difference in toughness obtained between the two media could then be attributed to water-driven fatigue. The K_{Ic} of ZT5-T was reduced 22% by indenting in H_2O and that of ZT5-M 21%. Details appear in Table III. It would seem that transformation toughening offers no special resistance to

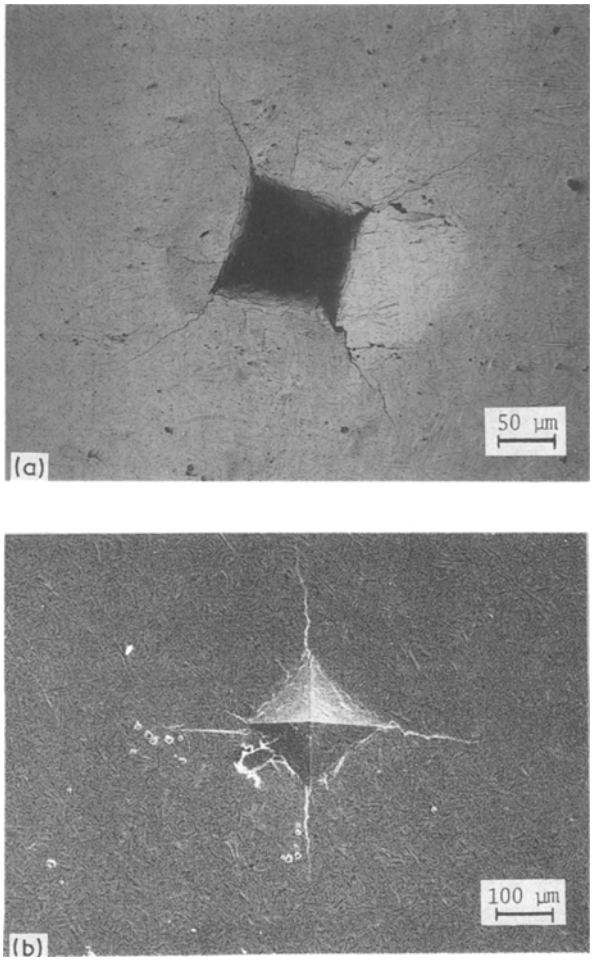

Figure 6 Scanning electron micrographs of (a) ZT5-T, and (b) ZT5-M. (Samples were indented with Vickers indentor using an indentation load of 196 N in paraffin oil.)

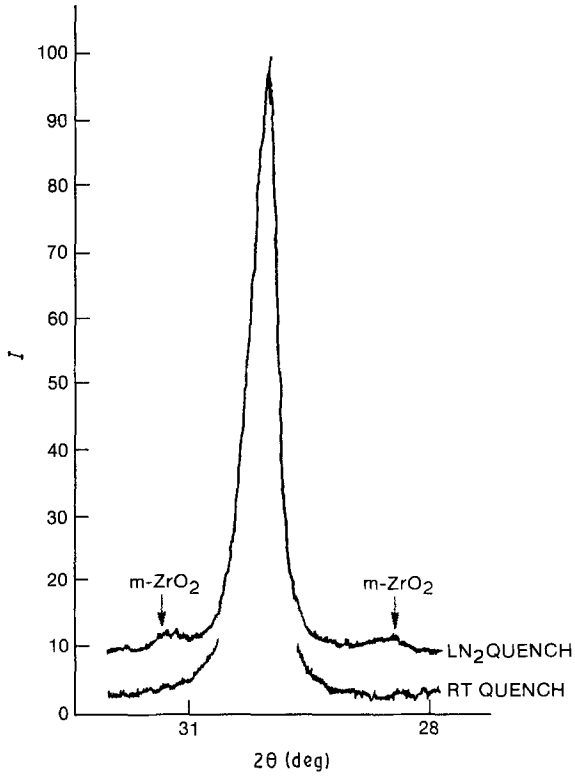

Figure 7 X-ray diffraction pattern of ZT5-T before and after exposure to 77 K. (Small peaks at 28.2° and 31.5° in liquid nitrogen-quenched sample indicate a partial transformation of t-ZrO_2 to m-ZrO_2.)

TABLE II SENB fracture toughness

Test condition	Toughness (MPa $m^{1/2}$)	
	ZT5-T (n*)	ZT5-M (n*)
25° C	2.29 ± 0.64 (33)	1.39 ± 0.64 (16)
77 K	1.64 ± 0.55 (15)	1.50 ± 0.40 (14)
Cooled to 77 K tested 25° C	1.59 ± 0.25 (15)	–

*n is the number of specimens tested

TABLE III Effect of H_2O on indentation fracture toughness

Test condition	Toughness (MPa $m^{1/2}$)	
	ZT5-T	ZT5-M
Paraffin oil	4.70 ± 0.70	2.90 ± 0.10
H_2O	3.67 ± 0.33	2.30 ± 0.29
% Reduction	21%	22%

fatigue in this system. However, the similar reductions in toughness may be due to the high reactivity of the lithium silicate matrix with water, rather than be indicative of any transformation-toughening response.

There is a significant difference in fracture toughness values obtained by indentation and values obtained from SENB. This is the result of the method used to determine toughness by indentation being only a relative measure of toughness and not an absolute method.

3.4. Transformation toughening

The K_{Ic} of ZT5-T is greater than that of ZT5-M by 0.9 MPa $m^{1/2}$. How much of this increase can be attributed to transformation toughening? The transformation zone size was determined to be ~ 1 μm. Assuming that the transformation dilation in this material is similar to an unconstrained transformation (a reasonable assumption given the large difference in elastic modulus between ZrO_2 and the lithium silicate matrix), the theoretical increment of toughening predicted by Equation 1 (using the following values: volume fraction t-ZrO_2 = 0.12, transformation strain = 0.0688, Young's modulus = 108 GPa, Poisson's ratio = 0.22, and transformation zone depth = 1 μm) is 0.2 MPa $m^{1/2}$, about 20% of the experimental value. In ceramics in which transformation toughening has been clearly established (i.e. partially stabilized zirconia, zirconia-toughened alumina) the toughening increment predicted by Equation 1 is usually 30% to 65% of the experimental value [7]. This estimate of toughening increase due to transformation toughening assumes an ideal transformation zone (i.e. a constant degree of transformation within the zone and no transformation outside the zone). Recent work has shown that, in general, transformation zones are not ideal [26, 27] (i.e. the concentration of transformed zirconia precipitates decreases with increasing lateral distance from the crack surfaces). This non-ideal zone is the result of the particle-size dependence of the martensitic t → m transformation and the stress gradient surrounding the crack tip. Hsueh and Becker [28] have shown that the presence of a non-ideal zone due to a particle-size distribution has a negligible effect on the toughening increment for narrow particle-size distributions, but the presence of wide particle-size distributions can result in a transformation-toughening increment of 20% (or more depending on the width of the distribution) higher than that calculated by assuming an ideal transformation zone. Transformation toughening then plays a fairly significant role in the improved toughness of ZT5-T. Microcrack weakening caused by the transformation of t-ZrO_2 to m-ZrO_2 upon cooling from the crystallization temperature in ZT5-M may account for a good portion of the remaining difference in toughness between ZT5-T and ZT5-M.

The small tetragonal zirconia crystallite size, 37 nm, of ZT5-T leads to questions about their "transformability" and ability to toughen by transformation toughening. Keefer and Michalske [17] found the t-ZrO_2 precipitates in their glass-ceramics to be of the order of micrometres and that only particles that intersected the crack would undergo transformation. Therefore, the transformation zone in their glass-ceramics is equal to the particle diameter. They attributed the stability of their particles to an absence of monoclinic nucleation sites; intersection with the crack generates monoclinic nucleation sites. The nuclei may be generated by actual fracture of the crystallite, the strain field of the crack, or by microcracking at the matrix/crystal interface. The only proviso of the model being that the range of these nucleation phenomena be small with respect to the crystallite size. Additionally, McCoy and Heuer [18] found in their system that the transformability of t-ZrO_2 precipitates depends on particle morphology. Regular-shaped particles lack nucleation sites for the martensitic transformation, whereas irregular-shaped particles could be transformed.

The observation of a transformation zone on the fracture surfaces of ZT5-T that is significantly larger than the average t-ZrO_2 particle size certainly suggests that the t-ZrO_2 precipitates in ZT5-T are very transformable. The transformation of some tetragonal zirconia in the glass-ceramic by cooling to liquid nitrogen also demonstrates this high degree of transformability. Further proof is found in that the maximum achievable average particle size of t-ZrO_2 found in this glass-ceramic system was rather small, 47 nm [20]. It also should be noted that the t-ZrO_2 precipitate size in calcia partially stabilized zirconia is of the same order of magnitude, ~ 80 nm at peak toughness and significant toughening at average precipitate sizes in the 40 to 50 nm range is observed [29].

Acknowledgements

The authors would like to acknowledge the support of Nippon Electric Glass Co. for this research (1984–1986). A part of this effort at Rensselaer was supported by the Army Research Office under contract no. DAAL03-89-K-0046.

References

1. R. C. GARVIE, R. H. HANNINK and R. T. PASCOE, *Nature* **258** (1975) 703.
2. N. CLAUSSEN, *J. Amer. Ceram. Soc.* **61** (1978) 85.
3. J. LORENZ, L. J. GAUCKLER and G. PETZOW, *Amer. Ceram. Soc. Bull.* **58** (1979) 338.

4. N. CLAUSSEN and J. JAHN, *J. Amer. Ceram. Soc.* **61** (1978) 94.
5. *Idem, ibid.* **63** (1980) 228.
6. R. M. McMEEKING and A. G. EVANS, *ibid.* **65** (1982) 242.
7. B. BUDIANSKY, J. W. HUTCHENSON and J. L. LAMBROPOULOS, *Int. J. Solid Struct.* **19** (1983) 337.
8. I. SAWAI, *Glass Technol.* **2** (1961) 243.
9. M. TASHIRO, *ibid.* **4** (1966) 428.
10. G. F. NEILSON in "Advances in Nucleation and Crystallization in Glasses", edited by L. L. Hench and S. W. Freiman (American Ceramic Society, Columbus, Ohio, 1971) pp.78–82.
11. D. R. STEWART, *ibid.*, pp. 83–90.
12. G. FAGHERAZZI, S. ENZO, V. GOTTARDI and G. SCARINCI, *J. Mater. Sci.* **15** (1980) 2693.
13. S. YOKOISHI and S. SAITO, *Yogyo-Kyokai-Shi* **88** (1980) 21.
14. G. H. BEALL and H. L. RITTLER, "Advances in Ceramics", Vol. 4, "Nucleation and Crystallization in Glasses", edited by J. H. Simmons, D. R. Uhlmann and G. H. Beall (American Society, Columbus, Ohio, 1982) pp. 301–12.
15. M. A. McCOY, W. E. LEE and A. H. HEUER, *J. Amer. Ceram. Soc.* **69** (1986) 292.
16. M. NOGAMI and M. TOMOZAWA, *ibid.* **69** (1986) 99.
17. K. D. KEEFER and T. A. MICHALSKE, *ibid.* **70** (1987) 227.
18. M. A. McCOY and A. H. HEUER, *ibid.* **71** (1988) 673.
19. D. R. CLARKE and B. SCHWARTZ, *J. Mater. Res.* **2** (1987) 801.
20. G. L. LEATHERMAN, PhD Thesis, Rensselaer Polytechnic Institute, Troy, New York (1986).
21. H. TORAYA, M. YOSHIMURA and S. SÔMIYA, *J. Amer. Ceram. Soc.* **67** (1984) C119.
22. H. P. KLUG and L. E. ALEXANDER, "X-Ray Diffraction Procedures for Polycrystalline and Amorphous Materials (Wiley, New York, 1974).
23. R. C. GARVIE, R. H. HANNINK and M. V. SWAIN, *J. Mater. Sci. Lett.* **1** (1982) 437.
24. B. R. LAWN and E. R. FULLER, *J. Mater. Sci.* **10** (1975) 2016.
25. K. TAKAHAGHI and A. OSAKA, *Yogyo-Kyokai-Shi* **91** (1983) 116.
26. P. F. BECHER and G. M. BEGUN, *Amer. Ceram. Soc, Bull.* **66** (1987) 520.
27. G. KATAGIRI, H. ISHADA, A. ISHITANI and T. MASAKI, *Mater. Res. Soc. Symp. Proc.* **78** (1987) 43.
28. C. H. HSUEH and P. F. BECHER, *J. Amer. Ceram. Soc.* **71** (1988) 494.
29. R. C. GARVIE, *J. Mater. Sci.* **20** (1985) 3479.

Received 19 May
and accepted 23 October 1989